Protection of Medical Images and Patient Related Information in Healthcare Using an Intelligent and Reversible Watermarking Technique

Muhammad Arsalan[1], Aqsa Saeed Qureshi[1], Asifullah Khan[*1], and Muttukrishnan Rajarajan[2]

[1]Department of Computer Science, Pakistan Institute of Engineering and Applied Sciences, Nilore-45650, Islamabad; asif@pieas.edu.pk

[2]School of-Mathematics, Computer Science and Engineering and, City University London, Northampton Square, EC1V 0HB, London, United Kingdom

Abstract

This work presents an intelligent technique based on reversible watermarking for protecting patient and medical related information. In the proposed technique 'IRW-Med', the concept of companding function is exploited for reducing embedding distortion, while Integer Wavelet Transform (IWT) is used as an embedding domain for achieving reversibility. Histogram processing is employed to avoid underflow/overflow. In addition, the learning capabilities of Genetic Programming (GP) are exploited for intelligent wavelet coefficient selection. In this context, GP is used to evolve models that not only make an optimal tradeoff between imperceptibility and capacity of the watermark, but also exploit the wavelet coefficient hidden dependencies and information related to the type of sub band. The novelty of the proposed IRW-Med technique lies in its ability to generate a model that can find optimal wavelet coefficients for embedding, and also acts as a companding factor for watermark embedding. The proposed IRW-Med is thus able to embed watermark with low distortion, take out the hidden information, and also recovers the original image. The proposed IRW-Med technique is effective with respect to capacity and imperceptibility and effectiveness is demonstrated through experimental comparisons with existing techniques using standard images as well as a publically available medical image dataset.

***Keywords*:** Health care, Integer Wavelet Transform, Genetic Programming, Reversible Watermarking, and Medical Images.

1. Introduction

The advancement in communication technologies has provided new ways of accessing and transferring the medical information. The widespread use of information and communication techniques

allows one to manipulate the original contents. Therefore, to protect the patient privacy and to ensure diagnostic accuracy, an effective medical image authentication mechanism is required without losing the semantics of the original content [33]. In this regard, digital watermarking has been advocated by many researchers as one of the most promising techniques to provide security, reliability, and authenticity of medical information [5].

Watermarking is considered as the practice of imperceptibility [16], changing a work to embed some information related to the work. Temper detection [22], copyright control [4], owner identification [6], broadcast monitoring [11], etc., are some of the interesting examples of watermarking applications. Generally, watermarking is categorized as Fragile, Robust, and Semi-fragile watermarking [10][20][7]. In fragile watermarking, alteration in image results in the destruction of watermark and robust watermarking aims to resist attacks [34][30]. Whereas in semi fragile watermarking, a watermark is supposed to resist unintentional attacks but get destroyed in case of intentional attacks.

The medical image watermarking is quite challenging and some essential constraints must be considered during the watermarking process. Embedding information in the host image causes distortion, which may be quite detrimental for medicalor military applications. A minute distortion in the medical image due to watermark embedding may turn it impracticable for the physicians. Therefore, there is a strong need to develop a watermarking technique that is not only able to embed the watermark but also able to restore the original content of the image after the watermark extraction. Reversible watermarking has the capability to restore the image back to the exact state, and thus fulfills the basic requirement [9]. An efficient reversible watermarking should be capable of embedding more information with fewer perceptual distortions as well as restoring the original image content. However, watermark capacity and imperceptibility are two contradicting properties, and therefore, it becomes a challenging task to make an optimal tradeoff between them for a given image and the intended application.

In medical image watermarking, one conventional way of protecting useful information in medical images is by defining a region of interest (ROI). The watermark is only embedded in ROI thus protecting the useful information from distortion [32]. However, in most scenarios the whole medical image has to be considered as ROI and embedding of information using ROI based approaches may not be acceptable.

This paper presents a block-based watermarking approach, in which the proposed IRW-Med utilizes the concept of companding for watermark embedding. Moreover, Genetic programming (GP) based intelligent coefficient selection is performed in integer wavelet domain, to exploit the inter-dependencies of wavelet coefficients.

The main leverage of this paper is in developing an intelligent embedding model for the given image, which has the following capabilities:

a) To make a suitable trade-off between capacity and imperceptibility of the watermark. Moreover to exploit the dependencies of wavelet coefficients and information regarding the type of sub bands.
b) To develop a model that not only helps in the selection of suitable coefficient for watermark embedding but also acts as the companding factor during embedding of the watermark.

In the proposed IRW-Med, block-based embedding helps not only in evolving mathematical expressions that select coefficients for companding through GP, but also acts as a threshold for companding. It is shown that for a given image (depending upon its frequency content), the learning ability of the GP makes it possible to find a suitable tradeoff between the watermark payload and imperceptibility. The optimal tradeoff between watermark imperceptibility and capacity is required in medical image watermarking for avoiding any misdiagnosis. The remaining portion of the paper is classified in the following way. Details regarding the proposed IRW-Med are described in Section 2. Results and performance analysis are discussed in Section 3. GP based implementation details are explained in section 4 and at the end the discussion related to conclusion is explained in Section 5.

2. Related Work

For decades researchers have put great efforts in the domain of reversible watermarking. Fridrich [13] proposed a lossless bit plane compression where extra space that is retrieved is used for the embedding of both the watermark and bookkeeping data. On the other hand, Alattar [1] proposed difference expansion to quads as a data hiding approach and achieved high capacity. Xuan et al. [26] proposed lossless approach related to data hiding based on Interger Wavelet Transform (IWT) and threshold based watermark embedding scheme. Xuan et al. [35], have also proposed a reversible and histogram shifting based watermarking technique, in which the information is embedded in the peak and neighborhood point by shifting the peak points towards zero point. Another work regarding reversible data hiding technique based on IWT is also proposed by Xuan [37]. Li et al. [19] proposed an adaptive

prediction error expansion based reversible watermarking technique. Another reversible watermarking technique based on prediction error is proposed by Coltuc et al. [8], in which the basic idea is to reduce the embedding distortion due to embedding of the prediction error. Lee et al. [18] proposed a genetic algorithm and particle swarm optimization based watermarking technique. Similarly, reversible watermarking is proposed by Arsalan [3], in which Genetic Algorithm evolves optimal/near optimal thresholds for companding. An interesting and effective watermarking technique is proposed by Sachenev et al. [25] using sorting and prediction. In their approach, only prediction error is used to embed watermark, whereas location map is rarely used. Dragoi et al. [12] proposed local prediction based on difference expansion. For copyright protection Gao et al. [14] reported histogram based technique, in order to add robustness,while An et al. [2] proposed histogram shifting and clustering based watermarking technique that is not only robust but also reversible. Siddiqa et al. [27] also proposed a watermarking technique which is reversible and dependent on the prediction error based expansion. In their approach, bits are embedded based on the scale of variation in the neighboring eight pixel values; however, there is no need for the location map or histogram shifting.

The challenging problem of making an optimal trade-off is still on-going and efforts for developing a model that can provide efficient trade-off for a given image are still being researched. In this context, the proposed IRW-Med addresses the shortcomings related to some of the recent existing methods; (a) To ensure reversibility, besides making an efficient tradeoff (for applications such as medical, military, and legal image based applications), (b) Recent intelligent approaches (especially, based on companding) concentrates on making a tradeoff or selecting suitable threshold, however, the companding function is not automatically handled. The proposed IRW-Med is able to automatically handle the companding function.

3. Proposed GP-IRW-Med approach

Like conventional watermarking, the proposed IRW-Med technique has two key phases; Embedding phase and Extraction phase. Proposed IRW-Med employs GP to evolve a mathematical function that selects the coefficients for companding. The general structural design of our proposed approach is based on the training phase (development of selection model of wavelet coefficients) and testing phase as shown in Fig. 1.

3.1 Developing GP based Selection Models for Medical Image Watermarking (Training Phase)

During GP simulation, the candidate expression is used to embed the watermark both with and without applying companding on the input image x. A fitness function evaluates the performance of each candidate expression and decides whether to keep the current expression for the next generation or discard it. Watermark payload and imperceptibility measures effect the fitness function. This procedure is repeated for all the individuals in a GP generation. After each generation, the fit individuals are elected as parents. New offsprings (candidate expressions) are produced from the parents by applying the genetic operators probabilistically. The procedure continues till a stopping criterion is reached, whereby the best GP expression, denoted by α, is saved. This comprises the training phase. In the testing phase, α is then used for watermark embedding. The following function is used for evaluating the fitness of a candidate expression,

$$Fitness = \begin{cases} 10 \times log_{10}\left(\frac{255^2}{MSE}\right) & \text{such that } effective\ `payload \geq \delta, payload \geq \beta \\ 0 & \text{Otherwise} \end{cases}. \quad (1)$$

Where δ and β are the desired effective-payload and the total payload respectively. MSE is the mean squared error between the original image, I and the watermarked image, I_w which is mathematically given as,

$$MSE = \frac{1}{M \times N} \sum_{i=0}^{M-1} \sum_{j=0}^{N-1} [I(i,j) - I_w(i,j)]^2. \quad (2)$$

3.1.1 Parameter setting of GP

GP is domain independent probability based algorithm, inspired by the biological evolution, mostly used for solving the optimization problems. Traditionally, GP represents a candidate solution in the form of a tree [17]. In order to represent the candidate solution, GP terminal and functional sets are defined. GP terminal set setting is shown in Table1 .

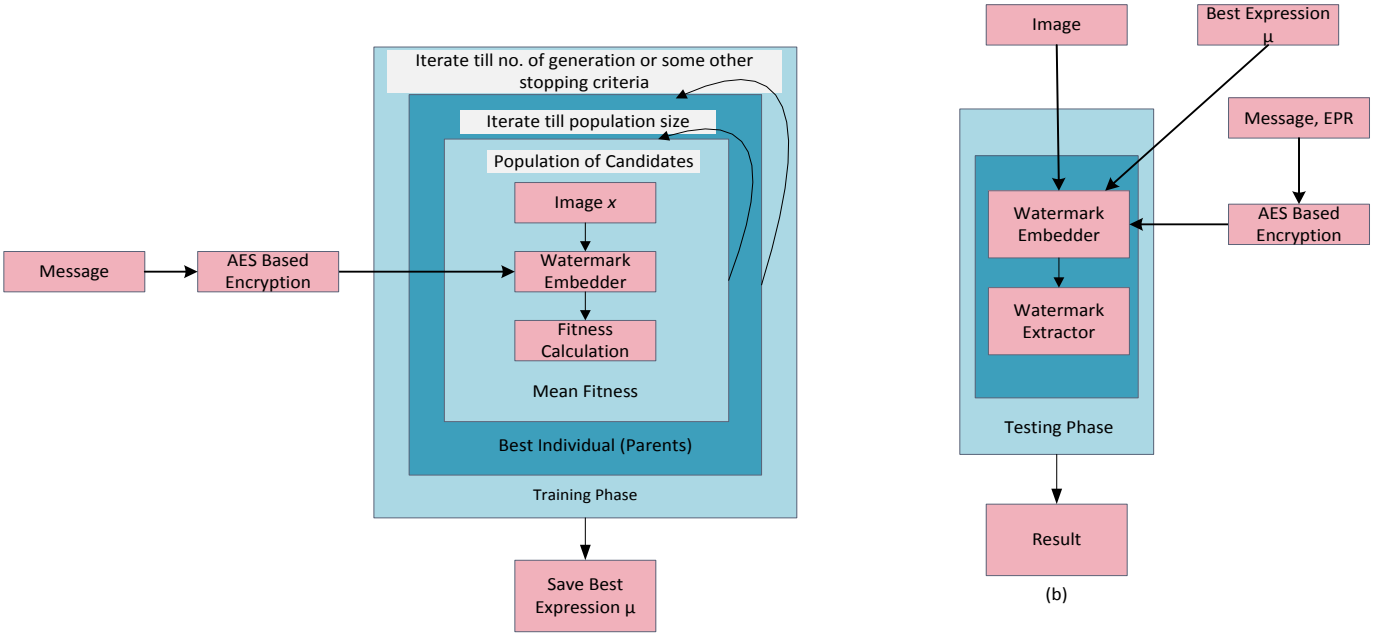

Figure 1: General Architecture of Proposed IRW-Med (a) training phase (b) testing phase

The aforementioned parameters of the terminal set assists GP in generating the suitable expressions by selecting appropriate coefficients and exploiting the neighborhood dependency on each other. Arithmetic operators (+, –, ×, and protected division), LOG, EXP, SIN, COS, MAX, and MIN form the GP function set.

Table 1 : Gp terminal set setting

Terminal Set	
Variable	Discription
Sub_{Label}	The mathematical value assigned to the different wavelet sub-bands used for embedding of watermark. We have assigned their value as LH=3, HL=4, HH=5.
Sub_{mean}	The average value of the coefficients in a specific sub-band.
Blc_{number}	Block position within a sub-band.
Blc_{mean}	The average value of coefficients in a block.
Blc_{max}	The maximum coefficient value in a block.
Blc_{min}	The minimum coefficient value in a block.
m,n	Stands for the row and column indices of the coefficient in block.

3.2 Medical Image Watermark Embedding and Extraction using the Best Evolved Model (Testing Phase)

In this phase, embedding and extraction are two main processes. The α (computed during the training phase) is used for the embedding of watermark in the testing phase. After the embedding of the watermark, next step is to make this embedding process reversible by extracting the watermark ensuring the full recovery of image to its original form along with the embedded watermark.

3.2.1 Embedding phase

During this phase, the watermark is generated first and then embedded into the original image. The watermark carries the patient information (EPR) along with the payload. Fig. 2 shows the steps involved in the embedding process.

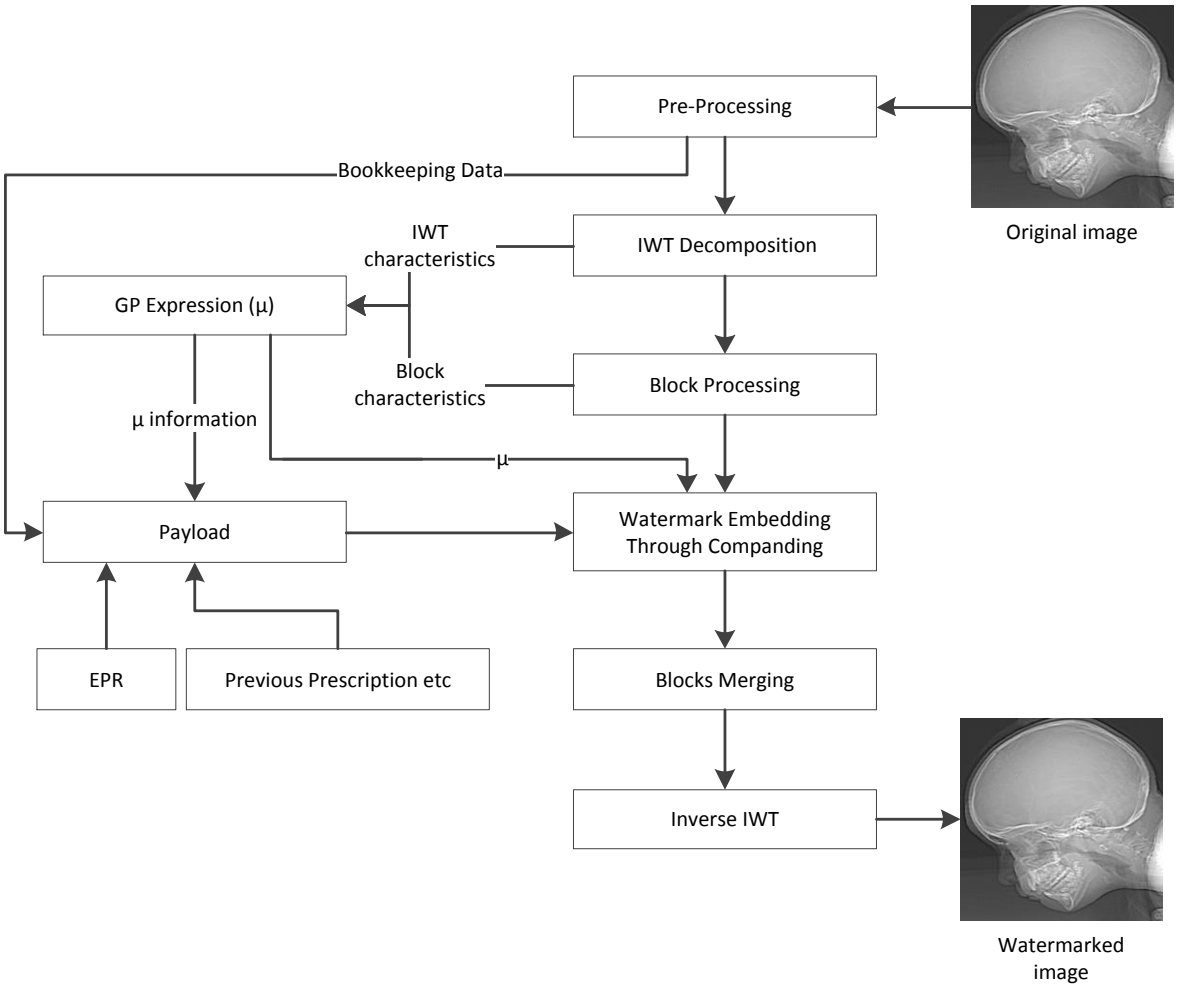

Figure 2: Block diagram of watermark embedding phase of the proposed IRW-Med technique

3.2.2 Pre-Processing and histogram modification

In most of the reversible watermarking approaches, some pre-processing is performed before embedding the watermark to overcome the potential problem of overflow and underflow. In proposed IRW-Med, histogram modification is applied before embedding the watermark to compress the histogram from both sides [36]. The Histogram modification process is explained with the help of a simple example as shown in Fig. 3. This figure shows the original and modified image obtained after the histogram modification. The range of the gray scale of original image is 0-255. Following the histogram modification, the range becomes 1-254. This is because after the modification the gray scale value 0 is

replaced by gray scale value 1 and gray scale 1 is replaced by gray scale value 2. Similarly, grayscale 255 is replaced by gray scale 254 and gray scale 254 is replaced by 253 respectively.

During the recovery phase, scan sequences are generated for obtaining the original image from histogram modified image. In histogram modified image all values of gray scale 1 and 254 are due to 0's and 255's in the original image. 2's in the modified histogram are because of 2's in the original image and 2's that are appeared by transforming 1's. In the same way, after modification all 253's are because of 253's in original image and 253's that are appeared by transforming 254's. That is why only for values of 2 and 253 scan sequences are created. For the generation of scan sequences, modified and original images are scanned simultaneously and if in both images the value at location (x, y) is 2, 1 is stored as a scan sequence otherwise, scan sequence is stored as 0. In a similar way, a scan sequence for gray scale 253 is generated. After generation of scan sequence Book keeping data store (BDS) is calculated as follows; BDS=BK+GC+LGS+L1+SC1+RGS+L2+SC2

Whereas;

BK=Total length of Book keeping data

GC= number of gray scales that are compressed

LGS=left hand side gray scales of first histogram

L1= record length

SC1= scan sequence

RGS= right hand side gray scale of first histogram

L2= record length

SC2=scan sequence

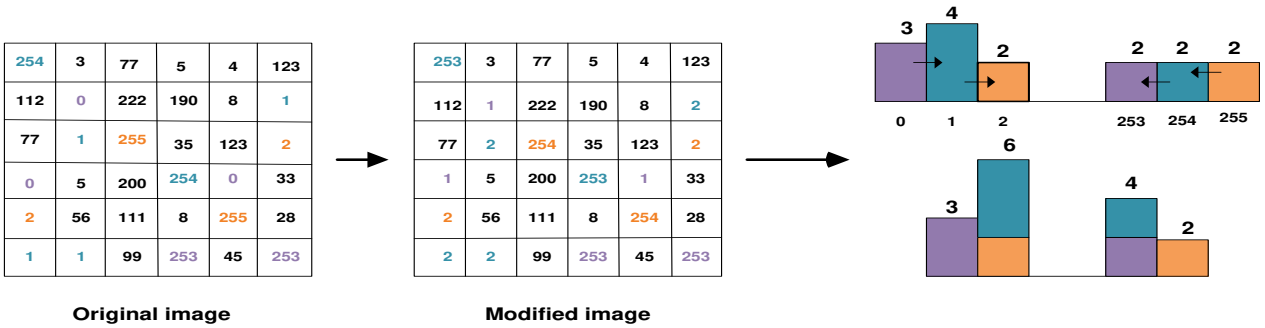

Figure 3: Histogram modification

The total length of bookkeeping data is the amount of bits required to store BDS. As grayscale 0 and 255 are compressed i.e., the number of gray scales that are compressed is two, so 4 or 8 bits are

needed for their storage. From the left hand side gray scale of first histogram is 1 which can be stored in 4 or 8 bits. The record length is the number of modified 2's in histogram and can be stored in 16 or 32 bits. This scan sequence of '2' is then appended. From the right-hand side the first histogram is gray scale 254 and this is stored in 8 bits. The record length of 253 is appended next followed by the scan sequence 253. All these pieces of information are combined together to form the BDS. The BDS information is stored as overhead and used in the histogram post-processing for recovering the original image after the extraction of the watermark.

3.2.3 Integer Wavelet Transform (IWT) of histogram-modified image

The second generation Cohen-Daubechies-Fauraue (CDF) IWT is employed for transforming the histogram-modified image into the frequency domain. CDF is employed because of greater capacity of embedding and improved visual appearance of watermark images. Moreover, CDF is integer to integer mapping; therefore, the round-off error remains zero, while applying the inverse transform.

After applying IWT on the image having size M x N, four sub-bands each having size $M/2 \times N/2$, are formed. These sub-bands represent frequency content within the image. It comprises of approximation (LL), horizontal (HL), vertical (LH), and diagonal detailed (HH) sub-bands [15]. The watermark is embedded in all sub-bands except LL sub-band to avoid the perceptual distortion, since the LL band offers high sensitivity to human visual systems.

3.2.4 GP based intelligent coefficient selection and companding

GP belongs to a class of biologically inspired optimization techniques. In GP, individual candidate solutions are produced and scored according to a fitness function. On the basis of fitness score, best individuals from the present generation are elected as parents for the next generation. The rest of the population is generated using the offspring produced, after randomly applying genetic operators on the parents. This process continues till a termination point is reached [26].

After IWT, the LH, HL, and HH bands are first divided into blocks of small dimension $m \times n$ and after that, an optimal/near-optimal GP expression is generated for the entire image. For every block, the value of the GP expression (when evaluated) varies because of its dependency on the characteristics of the block in question. This expression not only makes an efficient selection of the coefficient for companding but also decides how much companding of the coefficient has to be performed.

3.2.5 Intelligent companding based watermark embedding

Companding refers to a technique for compressing and then decompressing (or expanding) a signal. This process is generally used in reducing the data rate of audio signals for achieving high ratio

of signal to noise [36]. Companding applies compression to maps the signal from large to a narrow range, and then expansion restores the signal. The restored signal is very similar or same to the original one. Let θ and $\emptyset$ be the compression and expansion function respectively, and then companding is defined as;

$$\emptyset\big(\theta(x)\big) = x. \tag{3}$$

Eq. 3 is the sufficient and necessary condition to be satisfied for effectively applying the reversible watermarking technique.

Compression is applied for two purposes; firstly to reduce the scale of the resulting distortion (embedding the watermark in the signal avoid the overflow/underflow of the signal) and secondly, for achieving higher ratio for signal-to-noise [23].

The high frequency-coefficients of IWT in majority of the images follow distribution similar to Laplacian. According to Xuan et al.[36], distribution is related to two features:

- IWT coefficients having low magnitude don't require any compression, since embedding information in such coefficients will not cause them to underflow or overflow. A linear compression function having form $F(x) = x$ can be used for these coefficients.
- After embedding high magnitude coefficients have a high chance of overflow/underflow. So, it is more effective to use a function having steeper slope like the linear compression function.

Based on the aforementioned features, a piecewise linear function is used as shown in Eq. 4, where $\mu(i,j)$ denotes the value after applying α on a block $blck(i,j)$, *i.e.,* $\mu(i,j) = \alpha(block(i,j))$. Since α contains information regarding the suitable choice, therefore, the value of $\mu(i,j)$ decides which coefficient should be selected.

$$\theta_c(x) = \begin{cases} x, & |x| < \mu(i,j) \\ sign(x).\left(\left(\frac{|x|-\mu(i,j)}{2}\right) + \mu(i,j)\right), & |x| \geq \mu(i,j) \end{cases} \tag{4}$$

where x is the original wavelet coefficient and $\theta_c(x)$ is the compressed wavelet coefficient. The coefficients obtained after applying Eq. 4 may have values that lie in a continuous range. That is why quantization of compandding function is applied:

$$Q(\theta) = \theta_q(x) = \begin{cases} x, & |x| < \mu(i,j) \\ sign(x).\left(\left\lfloor \frac{|x| - \mu(i,j)}{2} \right\rfloor + \mu(i,j)\right), & |x| \geq \mu(i,j) \end{cases} \quad (5)$$

$$Q(\emptyset) = \emptyset_q(\theta_q(x)) = \begin{cases} \theta_q(x), & |\theta_q(x)| < \mu(i,j) \\ sign\left(\theta_q(x)\right).\left(2|\theta_q(x)| - \mu(i,j)\right), & |\theta_q(x)| \geq \mu(i,j) \end{cases} \quad (6)$$

In case of some signals, $\emptyset_q\left(\theta_q(x)\right) \neq x$, producing an error $r = \emptyset_q\left(\theta_q(x)\right) - x \neq 0$, which must be recorded for the recovery of IWT coefficients. Thus error r is embedded along with watermark into the host signal x. On the extraction side, the original coefficients are then recovered as follows:

$$x = Q(\emptyset) + r. \quad (7)$$

3.2.6 Data embedding

In the proposed IRW-Med technique, the watermark contains original message along with the bookkeeping data that is generated during histogram modification and the companding process. First, the compressed coefficients are represented in binary sequence and then least significant bits (LSBs) is used for watermark embedding. Suppose, the binary expression of the compressed coefficient is given by $y = b_1 b_2 b_3 \cdots b_n$, where $b_i \in \{0,1\}$. The watermark bit, w, is appended after LSB of y, and we get $Y = b_1 b_2 b_3 \cdots b_n w$. This can be written as $Y = 2 \times y + w$.

In the proposed IRW-Med technique, $\mu(i,j)$ is a critical value. It has a direct impact on the payload and watermarked image quality. Smaller value of $\mu(i,j)$ causes small alteration in the coefficients and consequently, good quality of marked images are attained, however, corresponding compression error will be large, resulting in reduction of the payload. When $\mu(i,j)$ is large, larger payload is achieved. However, the visual quality of the watermarked image will suffer due to large alteration in coefficients.

3.3 Extraction phase of the proposed IRW-Med technique

On the receiving side, the same procedure is applied to extract the watermark and original image but in a reverse direction. The extraction process is illustrated with a block diagram in Fig. 4.

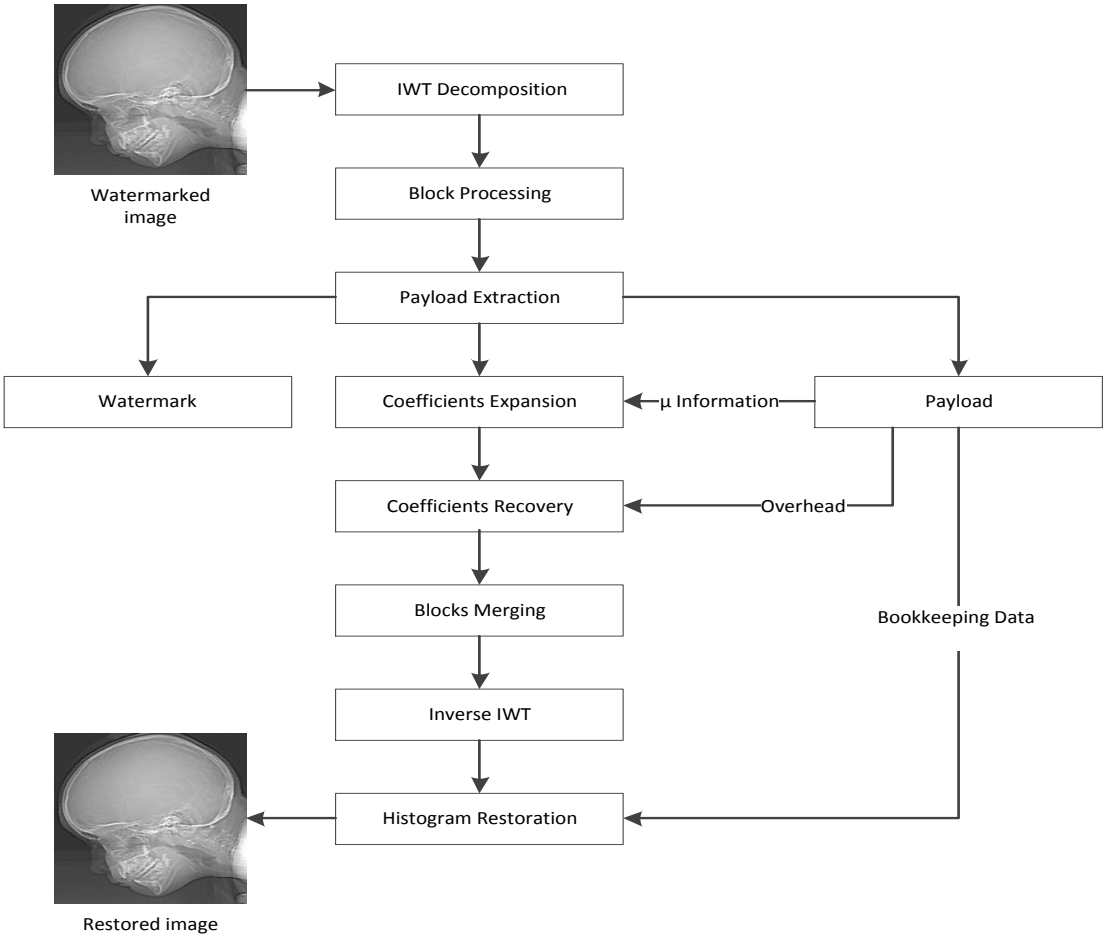

Figure 4: Block diagram showing extraction phase of the proposed IRW-Med

3.3.1 IWT of the received Image

For the extraction of watermarked image IWT is first applied to transfer the watermarked image to the wavelet domain. As a result, four wavelet sub-bands are obtained on which further processing is performed.

3.3.2 Wavelet coefficients recovery

The LSBs of the coefficients Y are extracted using $e = LSB(Y)$. To extract least significant bit from coefficients, modulus obtained after the division of coefficient by 2 returns the LSB which is either 1 or 0. For example, let 5 is the value of coefficient, in binary form we can express it as 0101. LSB in case of 5 is 1, so division of 5 by 2 returns 1 as modulus (Which is LSB). The extracted LSBs include the expression μ, original watermark, the overhead caused by the error in companding process, and the bookkeeping data created during histogram modification. The compressed coefficients are recovered

using μ and the overhead. Then, during expansion the error as well as overhead is used in the recovery of coefficients in the original form $x = \emptyset(x)$, while the bookkeeping data restores the histogram.

3.3.3 Image restoration

After extracting the data and recovering the original coefficients, inverse IWT restores the image to the spatial domain. Then, with the help of BDS, the histogram is restored. Scan sequences generated during histogram modification are used for the recovery of the histogram. Finally, the image is transformed into its original state.

4. Results and Discussion

The proposed IRW-Med approach is tested on various gray scale standard images such as Lena, Baboon, Barbara, and Gold hill as well as on standard medical images; the size of each image is of size 512×512. Matlab based GPLab toolbox has been utilized in order to develop a suitable GP expression. For Lena image best expression is presented in prefix notation as follows.

plus(multiply(subtract(subtract(log(log(0.27033)),mylog(protected-
division(blk_index,0.31993))),sin(log(blk_index))),subtract(sin(protected-
division(multiply(0.52962,blk_max),blk_max)),sin(blk_index))),blk_mean)

The corresponding GPLAB tree with the respective node labels for this expression is shown in Fig. 5. Fig. 6 shows the effect of embedding and extracting processes on the standard images. It illustrates the potential of our GP approach in embedding a high payload with small perceptual distortion. Column (a) in Fig. 6 presents the input images. They are subjected to watermark, using the best mathematical expression evolved through GP, and the outcomes are shown in column (b). Column (c) shows the dissimilarity between watermarked and the original image, indicating indiscernible embedding of the watermark by using the best evolved expression using GP simulations The naked eye is unable to differentiate this difference, so some amplification is done to enhance the difference as shown in column (d). After the extraction of the watermark, the contents of the image are recovered. The re-established images are revealed in column (e). The structural similarity index (SSIM) is used to show the performance of our proposed IRW-Med system in restoring the images. It is observed that for all the restored images in Fig. 6, the value of SSIM index is 1, when compared with their original images thus showing 100% restoration.

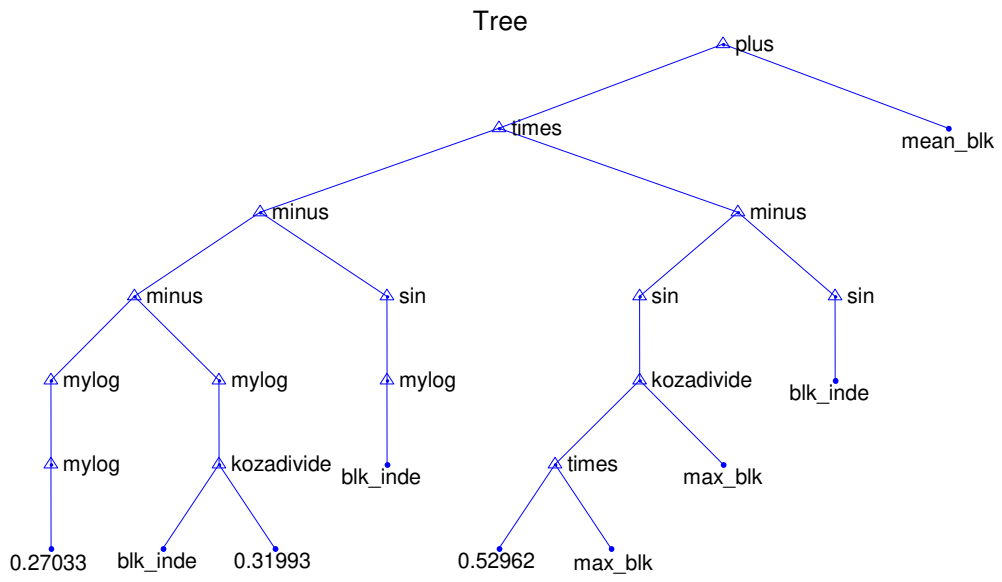

Figure 5: Tree of the evolved GP expression

4.1 Comparison with Existing techniques

Fig.7. compares the existing reversible watermarking techniques [36],[37],[28],[31],[18],[3],[35],[27],[25],[19],[8],[12] with the proposed IWT-Med. Tian's technique is quite interesting but its disadvantage is that for locating the expanded differences, extra information of location map is inserted besides the watermark in the image. This considerably degrades the image, in case there is no sufficient space for embedding the location map. Therefore, a suitable compromise between capacity and imperceptibility is needed to generate more gap for the overhead. Xuan [36] apply companding on coefficients using a fixed threshold. This companding is also applied on coefficients which do not need companding, or require companding but less or greater than the threshold producing unnecessary degradation in an image. Another disadvantage of the Xuan's approach is that the thresholding is performed using hit and trial method. Existing reversible watermarking techniques provide a useful tradeoff between capacity and imperceptibility of watermarked image [36],[37],[35],[28],[13]. However, there is still a margin of improvement that mainly depends on the selection of the threshold. Therefore, we exploit the learning capabilities of *GP* for automatically generating a mathematical expression that not only acts as a threshold but also as a companding factor in the companding process for a given image.

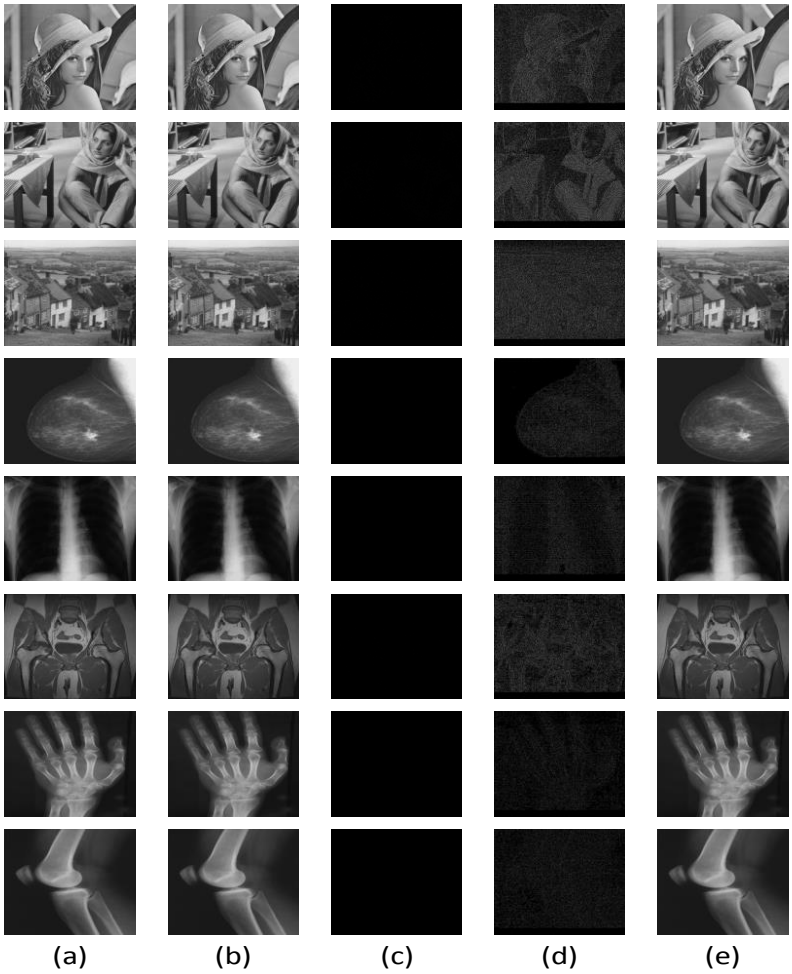

Figure 6: Embedding and extraction performance of the proposed IRW-Med on various images. Column (a) shows input images, (b) shows the watermarked images, (c) shows the difference of ((a) and (b)), (d) shows the amplified difference of (a) and (b), (e) shows the recovered image on the extraction side

In Fig. 7 for Lena image the compromise between payload and imperceptibility is shown. It is observed that the proposed IRW-Med yields better imperceptibility at higher payloads (0.4-0.7 bpp) compared to the existing schemes as shown in Fig. 7. This is accomplished by letting GP develop an optimal expression based on the coefficient magnitude, its location in the block, its neighborhood in the blocks, and the type of sub-band it belongs to. However, at lower payload (0.1-0.3bpp), the proposed IWT-Med shows comparable results to the existing reversible watermarking techniques, except Sachnev et al.'s technique [20] and GA-RevWM [3]. This is because in GA-RevWM, whereby GA is employed, the threshold selection is block-based, and therefore when the numbers of blocks are few, then GA performs better. Whereas in the proposed IWT-Med, the GP has to produce a generic expression applicable to all the blocks in the image, therefore, when the number of blocks (and correspondingly payload) is small, GP may not produce as good results as that of GA-RevWM [3].

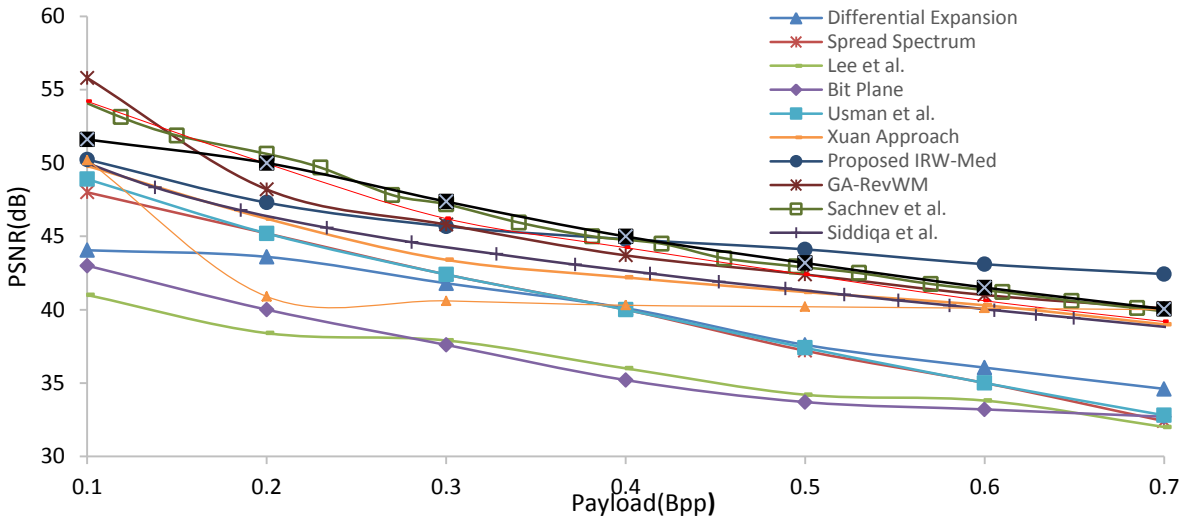

Figure 7: performance comparisons of Lena image in terms of Capacity vs. imperceptibility

4.2 Peak Signal-to-Noise Ratio (PSNR) vs. payload based performance comparison

Tables 2 and 3 present the performance comparison of the proposed IRW-Med at various capacity values with the threshold based reversible watermarking technique of Xuan et.al [36]. This comparison is performed on different standard images and different medical images, where PSNR and SSIM measures are used for the imperceptibility based performance assessment. To demonstrate further the effectiveness of the proposed method it is evaluated over a set of 300 gray scale images of size 256x256 shown in suplementray Table 1. It is noticed that the proposed IRW-Med attains better performance than the Xuan's scheme in terms of PSNR and SSIM. For an image of size 512×512, a payload of 1bpp shows that a total of 262,144 bits are to be inserted in the image. Our proposed scheme uses three out of four sub-bands for watermarking embedding, therefore the 0.75 bpp (total of 196608 information bits) is maximum payload that could be achieved. The results for medical images have been achieved by reserving the effective payload greater than 0.6bpp. The time complexity of the proposed method against Xaun approach is given in Table 4. The table show's the average time taken for both approaches against different payloads. The size of the image is kept at 256 x 256. These results are obtained on Matlab 2015(b) on Intel(R) Core(TM) i7-33770 CPU@3.4 GHZ with random access memory (RAM) of 16 GB. Moreover, the comparison of average of PSNR and standard deviation of 300 images of the proposed method with Xuan's approach [36] is shown in Table 5. The proposed approach out perform the Xuan's approach [36]. Since our proposed IRW-Med approach is capable of restoring the original image, therefore, we can make use of the entire image for information embedding without avoiding ROI. Fig. 8 shows the comparison of imperceptibility and payload of proposed IRW-Med with Xuan's

approach [36]. It is evident from the figure that the proposed IRW-Med yields better performance as compared to Xuan's [36] approach in the range of (0.0 - 0.7) bpp.

Table 2: PSNR (dB) vs. payload (bpp) based comparison of proposed IRW-Med with that of the Xuan's approach.[36]

Image	Payload (bpp)	0.1	0.2	0.3	0.4	0.5	0.6	0.7
Lena	Effective payload (bpp)	0.58						
	PSNR (dp) Xuan et al. [36]	49.8	46.2	43.4	42.2	41.2	40.3	39.0
	PSNR (dB) Proposed (IRW-Med)	50.86	46.71	45.2	44.3	43.6	42.6	41.87
Barbara	Effective payload (bpp)	0.48						
	PSNR (dp) Xuan et al. [36]	48.6	45.6	43.3	41.2	40.6	39.7	38.6
	PSNR (dB) Proposed (IRW-Med)	50.24	47.3	45.68	44.81	44.11	43.10	42.43
Goldhill	Effective payload (bpp)	0.4						
	PSNR (dp) Xuan et al. [36]	50.0	46.6	44.4	42.9	41.8	40.9	40.2
	PSNR (dB) (Proposed (IRW-Med))	52.59	49.26	47.92	46.67	46.22	44.83	44.11
X-ray	Effective payload (bpp)	>0.6						
	PSNR (dp) Xuan et al. [36]	53.8	50.0	48.1	46.0	45.6	44.8	44.1
	PSNR (dB) Proposed (IRW-Med)	54.43	50.70	49.03	48.11	47.28	46.29	45.53
Breast	Effective payload (bpp)	>0.6						
	PSNR (dp) Xuan et al. [36]	56.0	51.7	49.1	47.3	45.9	44.9	44.2
	PSNR (dB) Proposed (IRW-Med)	56.2	51.6	49.9	48.8	47.7	47.0	46.2
Belly	Effective payload (bpp)	>0.6						
	PSNR (dp) Xuan et al. [36]	51.29	47.97	45.96	44.32	43.17	42.38	41.70
	PSNR (dB) Proposed(IRW-Med))	52.12	48.94	47.37	46.55	45.83	44.93	44.20
Hand	Effective payload (bpp)	>0.6						
	PSNR (dp) Xuan et al. [36]	56.28	51.98	49.76	48.28	47.22	46.37	45.69
	PSNR (dB) Proposed (IRW-Med)	56.79	52.28	50.38	49.20	48.10	47.27	46.67
Knee	Effective payload (bpp)	0.58						
	PSNR (dp) Xuan et al. [36]	54.73	51.56	49.35	47.86	46.80	45.96	45.25
	PSNR (dB) Proposed(IRW-Med)	56.41	52.97	50.53	49.49	48.58	47.6	46.59

Table 3: Comparisons of SSIM of proposed IRW-Med technique against Xuan et al. approach [36], at different payload.

Image	Payload	0.1	0.2	0.3	0.4	0.5	0.6	0.7
	Effective payload (bpp)				0.58			
Lena	SSIM Xuan et al. [36]	0.9940	0.9881	0.9826	0.9776	0.9729	0.9682	0.9633
	SSIM (Proposed IRW-Med)	0.9939	0.9886	0.9836	0.9794	0.9783	0.9707	0.9707
	Effective payload (bpp)				0.48			
Barbara	SSIM Xuan et al. [36]	0.9966	0.9933	0.9896	0.9860	0.9830	0.9793	0.9744
	SSIM (Proposed IRW-Med)	0.9968	0.9943	0.9910	0.9890	0.9869	0.9832	0.9811
	Effective payload (bpp)				0.4			
Goldhill	SSIMXuan et al. [36]	0.9956	0.9918	0.9886	0.9851	0.9815	0.9786	0.9746
	SSIM (Proposed IRW-Med)	0.9976	0.9957	0.9937	0.9924	0.9915	0.9885	0.9869
	Effective payload(bpp)				>0.6			
X-ray	SSIM Xuan et al. [36]	0.9971	0.9928	0.9886	0.9843	0.9801	0.9760	0.9719
	SSIM (Proposed IRW-Med)	0.9971	0.9932	0.9903	0.9878	0.9853	0.9817	0.9783
	Effective payload (bpp)				>0.6			
Breast	SSIMXuan et al. [36]	0.9986	0.9960	0.9929	0.9895	0.9861	0.9831	0.9799
	SSIM (Proposed IRW-Med)	0.9983	0.9958	0.9936	0.9917	0.9896	0.9872	0.9854
	Effective payload (bpp)				>0.6			
Belly	SSIM Xuan et al. [36]	0.9955	0.9907	0.9863	0.9823	0.9781	0.9735	0.9683
	SSIM (Proposed IRW-Med)	0.9961	0.9927	0.9891	0.9872	0.9848	0.9813	0.9785
	Effective payload (bpp)				>0.6			
Hand	SSIM Xuan et al. [36]	0.9982	0.9953	0.9925	0.9896	0.9867	0.9837	0.9806
	SSIM (Proposed IRW-Med)	0.9984	0.9955	0.9927	0.9905	0.9876	0.9853	0.9836
	Effective payload (bpp)				0.58			
Knee	SSIM Xuan et al. [36]	0.9973	0.9943	0.9905	0.9867	0.9832	0.9794	0.9756
	SSIM(Proposed IRW-Med)	0.9981	0.9957	0.9925	0.9906	0.9879	0.9851	0.9819

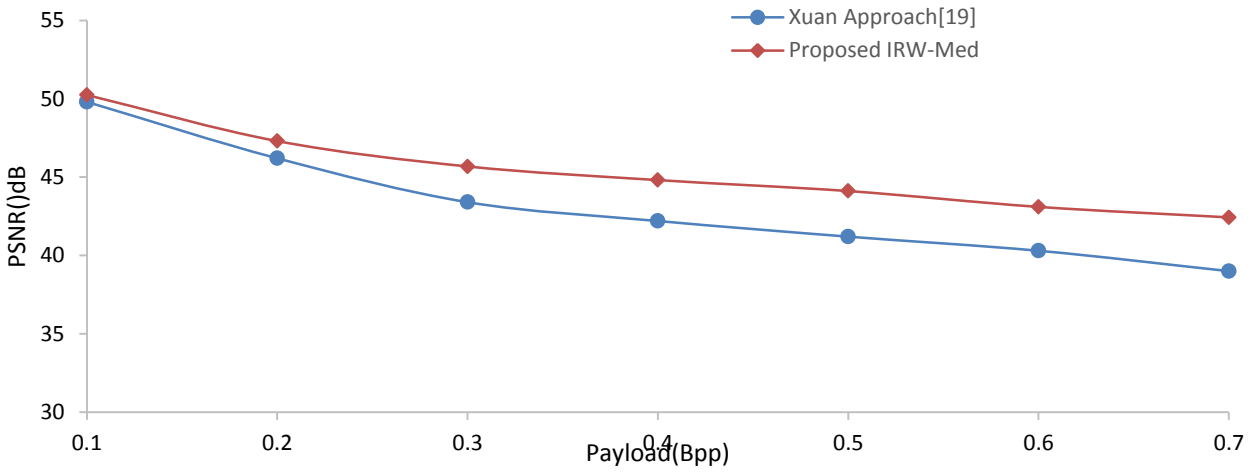

Figure 8: Comparison between proposed IRW-Med and Xuan's Approach for payload (0.1–0.7)

Table 4: Time complexity comparison of proposed method with Xuan et al. approach [36]

Payload	Average time in seconds Xuan's approach	Average time in seconds Of Proposed IWT-Med
0.1	0.6068	208.0176
0.2	0.6485	219.4836
0.3	0.6472	229.8939
0.4	0.7149	244.2717
0.5	0.7884	255.2785
0.6	0.8367	252.5790
0.7	0.8688	262.3846
0.75	0.9085	261.4694

Table 5: Average and standard deviation compasrion of 300 images of proposed method with Xuan et al. approach [36]

Payload	Xuan's Approach		Proposed IWT-Med	
	Average Value of PSNR	Standard Deviation of Error	Average Value of PSNR	Standard Deviation of Error
0.1	54.81	1.10	56.25	0.33
0.2	51.53	0.90	53.05	0.29
0.3	49.48	0.68	51.38	0.34
0.4	47.97	0.51	50.31	0.38
0.5	46.79	0.42	49.35	0.43
0.6	45.86	0.37	48.21	0.38
0.7	45.10	0.35	47.33	0.31
0.75	44.74	0.35	46.95	0.25

4.3 Embedding and Extraction of Electronic patient record (EPR)

This section explains the embedding of EPR data along with the watermark. The EPR data may include Patient ID (P_ID), Age of the patient, Gender (G), ID of the doctor (D_ID), Blood pressure (BP), level of Sugar (Sugar), and proposed Treatment (Recommended Treatment). Data is embedded in EPR in two different ways; one in the form of a binary picture as shown in Fig. 9 (a) and second; in the form of a string as shown in Fig. 10(a) [24]. The recovery of EPR in both of the forms on the extraction side is evident in the Figs 9(b) and 10(b), respectively [29][21].

Embedded EPR

EPR for John Wilson						
P_ID	Age	G	D_ID	BP mm Hg	Sugar Mg/dl	Recomended Treatment
0001	25	M	0109	100	99	IFA Test

(a)

Recovered EPR

EPR for John Wilson						
P_ID	Age	G	D_ID	BP mm Hg	Sugar Mg/dl	Recomended Treatment
0001	25	M	0109	100	99	IFA Test

(b)

Figure 9: (a) Embedded EPR on embedding side, (b) Recovered EPR on the extraction side

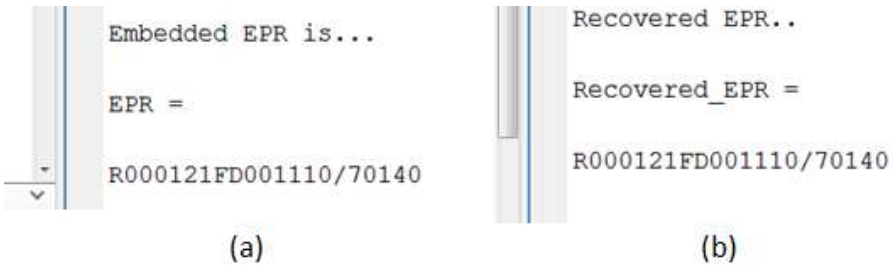

Figure 10: (a) EPR embedded in string form on embedding side, (b) EPR restored on the extraction side

4.4 Analysis of the evolved GP expression for Watermark Embedding

Fig. 11 shows the learning ability of the GP for generating a suitable expression for Lena image. The graph shows the variation in PSNR against the number of generations (up to 50 generations). It can be seen that in the start, PSNR values are zeros because the optimal expression produced during these generations are discouraged due to the following reasons.

1) The expression doesn't produce optimal value for companding in every block, rather increases the companding error as a result of effective payload becoming low.
2) The expression produces values out of threshold range.
3) The expression produced doesn't embed the whole watermark.

It can be observed from the Fig. 11 that after a few generations, learning ability of GP improves and produces a suitable expression for given PSNR value. This value of PSNR gets improved generation by generation.

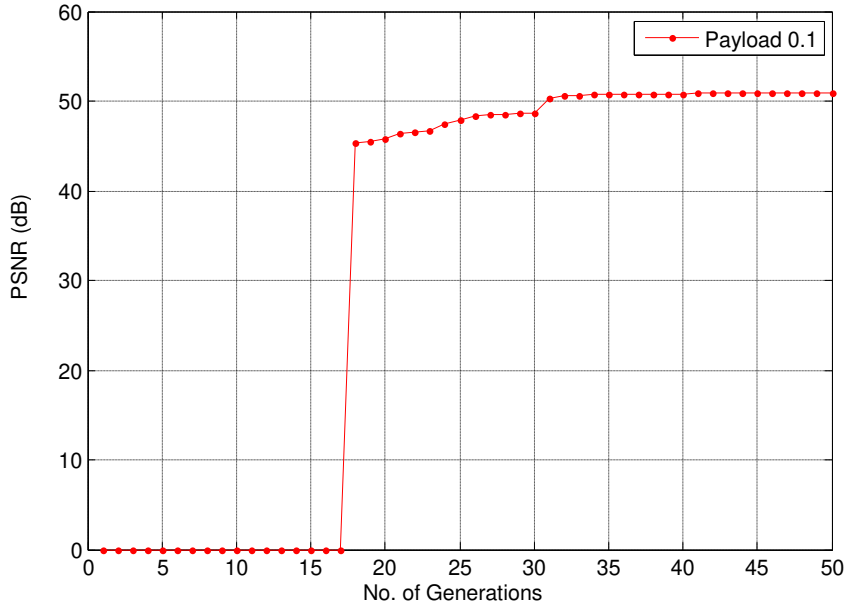

Figure 11: Learning ability of GP with generation

4.5 Implementation details and GP parameter setting

MATLAB is used to carry out simulations on different test images during the training phase. Initialization of population is carried out by Ramped-half and half method. Implementation details of all parameters used during simulations are summarized in Table 6.

Table 6: GP parameter setting

PARAMETER	**TYPE**
Function set	Rand, blk_indx, mean_blk, max_blk
Terminal set	Plus, minus, koza divide, exp, sin, cos, mylog
Expected number of offspring	Rank 89
Survival mechanism	Keep best
Type of mutation	Swap mutation
Sampling	Roulette
Operators probability type	Variable
Population in each generation	25
Number of generations	50

5. Conclusions

In this paper, reversible watermarking technique GP IRW-Med based on GP for protecting both the patient related information and associated medical image is proposed. Embedded watermark is based on the medical related information e.g., we have embedded EPR (Electronic patient record) as watermark, however embedding procedure is generic in nature.The capability of GP to learn is used to find suitable tradeoff between the imperceptibility and payload. GP exploits the hidden characteristics of wavelet coefficients to generate a mathematical expression that acts as a threshold in the companding process. The proposed IRW-Med technique is reversible so it lies in fragile Watermarking category. This means any alteration in the watermarked image will distort the watermark. Since the proposed technique is fragile, the extraction processing will be no longer reversible if any filter is applied. Our proposed IRW-Med technique shows better results as compared to GA-ReWM approach because GP intelligently evolves expression, which produces different values according to each of the different blocks. On the other hand, in case of GA-ReWM, global threshold matrix is used for embedding the watermark in the image. It has been observed that at given effective payload proposed IRW-Med provides improved imperceptibility for an image in comparison to existing reversible watermarking approaches.

ACKNOWLEDGMENT

This work is supported by the Higher Education Commission of Pakistan under NRPU Research Grant No. 20- 1624/R&D/10/4603 and ICTRDF/TR&D/2012/62.

References

[1] A.M. Alattar, Reversible watermark using the difference expansion of a generalized integer transform., IEEE Trans. Image Process. 13 (2004) 1147–1156.

[2] L. An, X. Gao, X. Li, D. Tao, C. Deng, J. Li, Robust reversible watermarking via clustering and enhanced pixel-wise masking, IEEE Trans. Image Process. 21 (2012) 3598–3611.

[3] M. Arsalan, S.A. Malik, A. Khan, Intelligent reversible watermarking in integer wavelet domain for medical images, J. Syst. Softw. 85 (2012) 883–894.

[4] F.M. Boland, Watermarking digital images for copyright protection, in: Fifth Int. Conf. Image Process. Its Appl., IEE, 1995: pp. 326–330.

[5] R. Caldelli, F. Filippini, R. Becarelli, Reversible Watermarking Techniques: An Overview and a Classification, EURASIP J. Inf. Secur. 2010 (2010) 1–19.

[6] Y.-H. Chen, H.-C. Huang, Coevolutionary genetic watermarking for owner identification, Neural Comput. Appl. 26 (2015) 291–298.

[7] Chi Kin Ho, Chang-Tsun Li, Semi-fragile watermarking scheme for authentication of JPEG images, in: Int. Conf. Inf. Technol. Coding Comput. 2004. Proceedings. ITCC 2004., IEEE, 2004: pp. 7–11 Vol.1.

[8] D. Coltuc, Improved Embedding for Prediction-Based, 6 (2011) 873–882.

[9] I. Cox, M.L. Miller, J.A. Bloom, Digital watermarking, (2001).

[10] I.J. Cox, J. Kilian, T. Leighton, T. Shamoon, Secure spread spectrum watermarking for images, audio and video, in: Proc. 3rd IEEE Int. Conf. Image Process., IEEE, 1997: pp. 243–246.

[11] G. Depovere, T. Kalker, J. Haitsma, M. Maes, L. De Strycker, P. Termont, et al., The VIVA project: digital watermarking for broadcast monitoring, Proc. 1999 Int. Conf. Image Process. (Cat. 99CH36348). 2 (1999) 202–205.

[12] I.-C. Dragoi, D. Coltuc, Local-Prediction-Based Difference Expansion Reversible Watermarking, IEEE Trans. Image Process. 23 (2014) 1779–1790.

[13] J. Fridrich, M. Goljan, R. Du, <title>Invertible authentication</title>, in: P.W. Wong, E.J. Delp III (Eds.), Photonics West 2001-Electronic Imaging, International Society for Optics and Photonics, 2001: pp. 197–208.

[14] X. Gao, L. An, Y. Yuan, D. Tao, X. Li, Lossless Data Embedding Using Generalized Statistical Quantity Histogram, 21 (2011) 1061–1070.

[15] R.C. Gonzalez, R.E. Woods, Digital Image Processing (3rd Edition), 2007.

[16] H. Huang, J. Pan, Y.-H. Huang, F.-H. Wang, K.-C. Huang, Progressive Watermarking Techniques Using Genetic Algorithms, Circuits, Syst. Signal Process. 26 (2007) 671–687.

[17] J.R. Koza, Genetic programming: on the programming of computers by means of natural selection, illustrate, MIT press, 1992.

[18] S. Lee, C.D. Yoo, T. Kalker, Reversible Image Watermarking Based on Integer-to-Integer Wavelet Transform, IEEE Trans. Inf. Forensics Secur. 2 (2007) 321–330.

[19] X. Li, B. Yang, T. Zeng, Efficient Reversible Watermarking Based on Adaptive Prediction-Error Expansion and Pixel Selection, 20 (2011) 3524–3533.

[20] E.T. Lin, E.J. Delp, E.T. Lin, E.J. Delp, A Review of Fragile Image Watermarks, (2001).

[21] N.A. Memon, S.A.M. Gilani, Adaptive data hiding scheme for medical images using integer wavelet transform, in: 2009 Int. Conf. Emerg. Technol., IEEE, 2009: pp. 221–224.

[22] Z. Parmar, A Review on Video / Image Authentication and Temper Detection Techniques, 63 (2013) 46–49.

[23] M.B. Pursley, Introduction to digital communications, (2005).

[24] S.C. Rathi, V.S. Inamdar, Analysis of watermarking techniques for medical images preserving ROI, in: Comput. Sci. Inf. Technol. (CS IT 05)-Open Access-Computer Sci. Conf. Proc., 2012: pp. 297–308.

[25] V. Sachnev, Hyoung Joong Kim, Jeho Nam, S. Suresh, Yun Qing Shi, Reversible Watermarking Algorithm Using Sorting and Prediction, IEEE Trans. Circuits Syst. Video Technol. 19 (2009) 989–999.

[26] Y.Q. Shi, Lossless Data Hiding Using Integer Wavelet Transform and Threshold Embedding Technique, in: 2005 IEEE Int. Conf. Multimed. Expo, IEEE, n.d.: pp. 1520–1523.

[27] A. Siddiqa, A. Khan, High capacity reversible image watermarking using error expansion and context-dependent embedding, Electron. Lett. 51 (2015) 985–987.

[28] J. Tian, Reversible Watermarking by Difference Expansion, Comp. A J. Comp. Educ. (2002) 19–22.

[29] M. Ulutas, G. Ulutas, V. V. Nabiyev, Medical image security and EPR hiding using Shamir's secret sharing scheme, J. Syst. Softw. 84 (2011) 341–353.

[30] I. Usman, A. Khan, BCH coding and intelligent watermark embedding: Employing both frequency and strength selection, Appl. Soft Comput. J. 10 (2010) 332–343.

[31] I. Usman, A. Khan, A. Ali, T.-S. Choi, Reversible watermarking based on intelligent coefficient selection and integer wavelet transform, Int. J. Innov. Comput. Inf. Control. 5 (2009).

[32] A. Wakatani, Digital watermarking for ROI medical images by using compressed signature image, in: Proc. 35th Annu. Hawaii Int. Conf. Syst. Sci., IEEE Comput. Soc, 2002: pp. 2043–2048.

[33] Weijian Xu, Hui Huang, Wenxue Yu, A study of medical image tampering detection, in: 2010 Int. Conf. Med. Image Anal. Clin. Appl., IEEE, 2010: pp. 131–134.

[34] X. Wu, W. Sun, Robust copyright protection scheme for digital images using overlapping DCT and SVD, Appl. Soft Comput. J. 13 (2013) 1170–1182.

[35] G. Xuan, Y. Shi, Z. Ni, Lossless data hiding using integer wavelet transform and spread spectrum, in: IEEE Int. Work. Multimed. Signal Process., Siena, 2004.

[36] G. Xuan, C. Yang, Y. Zhen, Y.Q. Shi, Z. Ni, Reversible Data Hiding Using Integer Wavelet Transform and Companding Technique, in: Digit. Watermarking, Springer, 2005: pp. 115–124.

[37] G. Xuan, J. Zhu, J. Chen, Y.Q. Shi, Z. Ni, W. Su, Distortionless data hiding based on integer wavelet transform, Electron. Lett. 38 (2002) 1646.